

# INVESTIGATION OF ZERO-SOUND DISPERSION EQUATION IN THE COMPLEX PLANE OF FREQUENCY

V.A. Sadovnikova  
Petersburg Nuclear Physics Institute,  
Gatchina, St. Petersburg 188300, Russia

## Abstract

The known solutions to the zero-sound dispersion equation are considered as placed on the physical and unphysical sheets in the complex plane of frequency.

## I. Introduction

In this paper we present the known solutions to the zero-sound dispersion equation obtained in the Landau kinetic theory [1]-[3] and in the microscopic theory in RPA [3]-[4] in the complex plane of frequency. The solutions are calculated for the different values of coupling constant and considered on the physical and unphysical sheets.

In recent years a large attention is paid to the problem of stability of the nuclear matter and the phase transitions in it [5], [6], [7]. To investigate the phase transitions, it is useful to understand what kind of excitations becomes amplified and leads to instability of matter with the changing of the temperature or density or coupling constant. In the fermi-liquid the amplified solutions appear at  $F_0 < -1$ . When we take into account the meson exchange then the zero-sound modes undergo the drastic modifications and the damping solutions can turn into the amplified ones and lead to the appearance of the instability of the description of nuclear matter.

In this note the solutions to the zero-sound dispersion equation are presented. They are given in such a form that permits to trace the influence of the external field and meson exchange on these solutions later on.

Following the papers [2], [4] we write the dispersion equation in the form

$$1 = \mathcal{F}\Pi^{0R}(\omega, k). \quad (1)$$

In this equation  $\mathcal{F}$  is the effective quasiparticle interactions,  $\omega$  and  $k$  are the frequency and the wave vector of the excitations. The operator  $\Pi^{0R}(\omega, k)$  is the retarded zero order on the quasiparticle interaction self-energy part (polarization operator). There is a known analytical expression for this polarization operator [2]-[4].

It was shown in papers [2], [5], that the energies of the zero-sound collective excitations are the poles of the two-quasiparticle Green function over the quasiparticle-quasihole channel. The two-quasiparticle Green function  $G^{(2)}$  is determined through the single-quasiparticle Green function  $G^{(1)}$  and the vertex function  $\Gamma$

$$G^{(2)} = G^{(1)}G^{(1)} + G^{(1)}G^{(1)}\Gamma G^{(1)}G^{(1)}.$$

When we consider the interacting quasiparticles near the Fermi surface with the small momenta transmitted then the vertex function  $\Gamma$  can be given by [5]

$$\Gamma(\omega, k) = \frac{1}{a^2} \frac{\mathcal{F}}{1 - \mathcal{F}\Pi^{0R}(\omega, k)}, \quad (2)$$

where  $a$  is a residue in the pole of  $G^{(1)}$ . In this equation the constant interaction between the quasiparticles is supported. On the other hand,  $\Gamma$  is the two-particle scattering amplitude that satisfy to the two-particle equation like Bethe-Salpeter one for the particle and hole [2].

The analytical singularities of the two-particle scattering amplitude in the complex plane of frequency are well known [8]. On the real axis of the physical sheet of  $\omega$  the stable excitations and cuts are placed. The cuts correspond to the excitation of the free particle-hole pairs. The damping excitations (resonances) are disposed on the unphysical sheets under the cuts. Besides, in the fermi-liquid at a strong attraction between quasiparticles  $F_0 < -1$  the imaginary solutions to the Eq.(1) appear. They are situated on the positive and negative imaginary axes of the physical sheet. These solutions break the causality conditions and point out the phase transition in nuclear matter. In the present paper we consider the stable, damping and increasing solutions of Eq.(1) for the different magnitudes of the quasiparticle interaction.

Following to [3], [8] we determine the physical sheet of the complex plane of frequency on which the stable solutions of Eq.(1) are situated. At some values of  $\mathcal{F}$  the solutions are placed both on physical and unphysical sheets. These unphysical sheets belong to the frequency Riemann surfaces that are determined by the form of  $\Pi^{0R}(\omega, k)$ .

We take  $\mathcal{F}$  as a constant scalar interaction  $\mathcal{F} = F_0 C_0$ . Here  $C_0$  is a factor inversed to the level density on the Fermi surface for two kinds of nucleons,  $C_0 = \pi^2/(2mp_F)$ .  $F_0$  is a dimensionless coupling constant of the scalar quasiparticle interaction.

We consider Eq.(1) in the kinetic theory of Landau [2]-[3] and in the microscopic theory in the random phase approximation (RPA) [2]-[4]. The results of these theories coincide at the long wavelenths. For the fixed  $F_0$  and Fermi momenta  $p_F$ , the solutions to Eq.(1) are the linear functions of the frequency  $\omega$  on the wave vector  $k$ :  $\omega = ks\frac{p_F}{m}$  in the kinetic theory. In RPA there is a more composite dependence, and we have branches of solutions  $\omega(k)$ .

In Sect.2 the analytical continuation of  $\Pi^{0R}(\omega, k)$  on the unphysical sheets of the complex plane is realized.

In Sect.3 the solutions of Eq.(1) for the attractive interaction  $F_0 < 0$  are presented. It is shown that the part of solutions to (1) is situated on the unphysical sheets (sheets  $I$  and  $I'$ ).

In Sect.4 the solutions for the repulsive interaction  $F_0 > 0$  are presented. It is shown how after the overlapping of the frequency of the zero-sound excitations,  $\omega_s(k)$ , and the

particle-hole continuum, the branch  $\omega_s(k)$  goes to the unphysical sheet (sheets  $II$  and  $II'$ ).

In the paper we consider the symmetric nuclear matter at zero temperature and the equilibrium density  $\rho = \rho_0$ ,  $p_F = 0.268$  GeV. During the computations the mass of the quasiparticles is taken equal to  $m = 0.8m_0$  and  $m_0 = 0.94$  GeV.

## II. The structure of polarization operator

In this section the expression for a polarization operator is given. The formulae repeat the known expressions [4], [3]. But they are presented in a form that is more convenient for the analytical continuation of  $\Pi^{0R}(\omega, k)$  in  $\omega$  from the physical on unphysical sheets. At the beginning we consider the expression for the polarization operator in RPA.

Recall that there is a condition on the magnitude of the retarded operator  $\Pi^{0R}(\omega, k)$  in the complex plane of  $\omega$  [2]

$$\Pi^{0R}(-\omega^*) = (\Pi^{0R})^*(\omega). \quad (3)$$

The expression for  $\Pi^0$  is taken from [3]-[4]. Let us write it in the form that does not content the overlapping logarithmic cuts. The causal operator  $\Pi^0$  can be presented as a sum of two terms. One term describes the excitation of the particle-hole pair in the medium and the second one corresponds to absorption of it

$$\Pi^0(\omega, k) = \phi(\omega, k) + \phi(-\omega, k). \quad (4)$$

For the real  $\omega$ , the retarded polarization operator is determined by the following way [4]

$$\Pi^{0R}(\omega, k) = (Re + i \text{sign}(\omega)Im)\Pi^0(\omega, k).$$

The expression for  $\phi(\omega, k)$  is written for the excitations in nuclear matter consisting of two sorts of nucleons with two spin projection.

For the wave vectors  $0 \leq k \leq 2p_F$  the term  $\phi(\omega, k)$  has a form

$$\begin{aligned} \phi(\omega, k) = & -4 \frac{m}{k} \frac{1}{4\pi^2} \left( \frac{-\omega m + kp_F}{2} - \omega m \ln \left( \frac{\omega m}{\omega m - kp_F + \frac{1}{2}k^2} \right) \right. \\ & \left. + \frac{(kp_F)^2 - (\omega m - \frac{1}{2}k^2)^2}{2k^2} \ln \left( \frac{\omega m - kp_F - \frac{1}{2}k^2}{\omega m - kp_F + \frac{1}{2}k^2} \right) \right). \end{aligned} \quad (5)$$

For  $k \geq 2p_F$  the term  $\phi(\omega, k)$  is a Migdal's function [5]:

$$\phi(\omega, k) = -4 \frac{1}{4\pi^2} \frac{m^3}{k^3} \left[ \frac{a^2 - b^2}{2} \ln \left( \frac{a+b}{a-b} \right) - ab \right], \quad (6)$$

where  $a = \omega - (\frac{k^2}{2m})$ ,  $b = \frac{kp_F}{m}$ .

Consider the cuts of  $\Pi^0(\omega, k)$  in the complex plane of  $\omega$ . From (5) we see that there are two cuts for  $k \leq 2p_F$  (denote them  $I$  and  $II$ ). They are determined by the first and the second logarithms in (5) and are placed on the real axis at  $\omega$  equal to

$$I : 0 < \omega < \frac{kp_F}{m} - \frac{k^2}{2m} \quad II : \frac{kp_F}{m} - \frac{k^2}{2m} < \omega < \frac{kp_F}{m} + \frac{k^2}{2m} . \quad (7)$$

It is easy to see that  $\phi(\omega, k)$  (5) is finite in the branch point  $\omega m = kp_F - \frac{1}{2}k^2$  due to the cancelation of the infinite contributions of the first and the second logarithms.

The cuts  $I$  and  $II$  can be considered as corresponding to the excitations of the different particle-hole pairs. The cut  $I$  describes the excitation of a hole with the energy  $\varepsilon_{\vec{p}_F - \vec{k}}$  and a particle on the Fermi surface. Then  $\omega = \frac{p_F^2}{2m} - \frac{(\vec{p}_F - \vec{k})^2}{2m}$  and the points of the cut correspond to the change of the angle  $\theta$  between  $\vec{p}_F$  and  $\vec{k}$  in the interval  $\frac{k}{2p_F} < \cos\theta < 1$ . The cut  $II$  describes the excitation of a particle with the energy  $\varepsilon_{\vec{p}_F + \vec{k}}$  and a hole on the Fermi surface. Then  $\omega = \frac{(\vec{p}_F + \vec{k})^2}{2m} - \frac{p_F^2}{2m}$  and the points of the cut correspond to  $1 - \frac{k}{p_F} < \cos\theta < 1$ .

The cuts of the function  $\phi(-\omega, k)$  lie on the negative real axis symmetrically with respect to the cuts of  $\phi(\omega, k)$ . Thus,  $\Pi^0(\omega, k)$  has four cuts in the complex plane of  $\omega$  which are shown in Fig.1a. When  $\omega > 0$  then the cuts stem from  $\phi(\omega, k)$  while for  $\omega < 0$  they are caused by  $\phi(-\omega, k)$ .

For the both of the logarithms in (5) the infinite-sheeted Riemann surface can be construct [9]. The logarithms are the single-valued function in it.

When  $k$  grows, approaching  $2p_F$ , cut  $I$  becomes shorter and degenerates into a point at  $k = 2p_F$ . For  $k > 2p_F$  there are two cuts on the real axis in Eq.(4):  $III$  and symmetrical  $III'$ .

$$III : -\frac{kp_F}{m} + \frac{k^2}{2m} < \omega < \frac{kp_F}{m} + \frac{k^2}{2m} . \quad (8)$$

Now we define the physical sheet according to the papers [2], [3]. In the long wavelenths limit  $k \rightarrow 0$ ,  $\frac{\omega}{k} \rightarrow const$ ,  $\Pi^0(\omega, k)$  (4) has a form

$$\Pi^0(\omega, k) \approx -4\frac{m}{k} \frac{1}{4\pi^2} \left( \frac{-\omega m + kp_F}{2} - \omega m \ln \left( \frac{\omega m}{\omega m - kp_F} \right) \right) \quad (9)$$

$$\begin{aligned} &+ \frac{\omega m + kp_F}{2} - \omega m \ln \left( \frac{-\omega m - kp_F}{-\omega m} \right) + kp_F \Big) \\ &= -2\frac{mp_F}{\pi^2} \left( 1 - \frac{\omega m}{2kp_F} \ln \frac{\frac{\omega m}{kp_F} + 1}{\frac{\omega m}{kp_F} - 1} \right) . \end{aligned} \quad (10)$$

We accept that on the physical sheet the logarithm in (10) has an imaginary part on the upper edge of the cut equal to  $-\pi i$  [3] and, consequently,  $+\pi i$  on the lower edge.

The corresponding retarded  $\Pi^{0R}$  is (we denote  $s = \frac{\omega m}{kp_F}$ )

$$\Pi^{0R} = 2\frac{mp_F}{\pi^2} \left( -1 + \frac{s}{2} \left[ \ln \left| \frac{s+1}{s-1} \right| - i\pi\theta(1 - |s|) \right] \right) . \quad (11)$$

Substituting Eq.(10) in (1) we obtain the known form of the zero-sound dispersion equation in the kinetic theory

$$1 + \frac{1}{F_0} = \frac{\omega m}{2kp_F} \ln \left( \frac{\omega m + kp_F}{\omega m - kp_F} \right) = \frac{s}{2} \ln \frac{s+1}{s-1}. \quad (12)$$

In Eq.(11) there is a cut on the real axis for  $(-\frac{kp_F}{m} < \omega < \frac{kp_F}{m})$ . Looking at Eq.(9) we consider this cut as consisting of two cuts  $I$  and  $I'$  (Fig.1a). At the long wavelenths Eq.(7) comes to  $I : 0 < \omega < \frac{kp_F}{m}$ .

### III. Solutions at $F_0 < 0$

In this section we consider solutions to Eqs.(1) and (12) at  $F_0 < 0$  in the complex plane of  $\omega$ .

The family of solutions to Eqs.(1) and (12) at  $F_0 < 0$  we denote by  $\omega_{sd}$ . The letters "sd" are connected with the words "spinodal decomposition". It is known [2] that the thermodynamic stability condition says that the matter is stable if the partial derivative of the pressure with respect to the volume is negative:  $(\frac{\partial P}{\partial V})_T < 0$ . The process which takes place in matter, when this condition is broken, is known as spinodal decomposition [7]. It is shown in [2] that there is a relation of the effective quasiparticle interaction to the partial derivative

$$\frac{\partial P}{\partial V} = -\frac{N}{V^2} \frac{p_F^2}{3m} (1 + F_0).$$

( $N$  is the number of particles). The stability condition is broken at  $F_0 < -1$ . It looks reasonable to use the notation  $\omega_{sd}(k)$  for the solutions at  $F_0 < -1$ . It is shown in this section that all solutions at  $F_0 < 0$  can be considered as belonging to the same family since they continuously turn one into another at the continuous change of  $F_0$ . Therefore the notation  $\omega_{sd}(k)$  is used for all solutions at  $F_0 < 0$ .

#### III.A The definition of the unphysical sheets

Let us turn to Eqs.(4) and (5) and define the unphysical sheets in the complex plane of  $\omega$ . Consider the cut  $I$ . We denote the first logarithm in (5) as  $\ln(z_1) \equiv \ln \left( \frac{\omega m}{\omega m - kp_F + \frac{k^2}{2}} \right)$ . While the frequency  $\omega$  goes along the cut  $I$  (7):  $\omega = (0, \frac{kp_F}{m} - \frac{k^2}{2m})$  then  $z_1$  is changed in the interval  $z_1 = (0, -\infty)$ . The cut  $I$  in the complex plane of  $\omega$  corresponds to the cut along the negative real axis in the complex plane of  $z_1$  (Fig.1b). When we go to the cut  $I$  from above (the arrow in Fig.1a), this corresponds that we go to the cut from below in the complex plane of  $z_1$  (the arrow in Fig.1b). Going over under the cut in Fig.1b we pass on to the unphysical sheet neighboring with the physical one on the Riemann surface of  $\ln(z_1)$ . The magnitudes of  $\ln(z_1)$  on the neighboring sheet differ by a quantity of  $(-2\pi i)$  from the magnitudes on the physical sheet at the same  $z_1$ .

Thus, going over under the cut  $I$  in Fig.1a we pass on to the unphysical sheet of the complex plane of  $\omega$  that is placed under the physical sheet. Let us denote the unphysical

sheet with the same letter as a cut:  $I$ . The magnitude of  $\ln\left(\frac{\omega m}{\omega m - kp_F + \frac{k^2}{2}}\right)$  on the sheet  $I$  differ from the magnitudes on the physical sheet by the quantity of  $(-2\pi i)$ . As example, the value of  $\ln\left(\frac{\omega m}{\omega m - kp_F + \frac{k^2}{2}}\right)$  on the lower edge of cut  $I$  is  $\ln\left(\frac{\omega m}{\omega m - kp_F + \frac{k^2}{2}}\right) + \pi i$ . But the value at the same point of  $\omega$  on the unphysical sheet is  $\ln\left(\frac{\omega m}{\omega m - kp_F + \frac{k^2}{2}}\right) - \pi i$ . Thus, we have the continuous changing of logarithm along the arrow in Fig.1a. Then we conclude that  $\Pi^{0R}$  in Eq.(1) changes continuously as well. The part of the unphysical sheet  $I$  is shown in Fig.1c by the shading with the right slope.

An important remark is that moving on the frequency Riemann surface of one of logarithms we stand on the physical sheet for the other logarithms. In another words, the Riemann surfaces of logarithms in Eq.(4) are independent.

Now we define an unphysical sheet related to the cut  $I'$  (denote the sheet by  $I'$ ). The cut  $I'$  stems from the first logarithm in  $\phi(-\omega, k)$ . We designate  $\ln(z'_1) \equiv -\ln\left(\frac{-\omega m}{-\omega m - kp_F + \frac{k^2}{2}}\right) = \ln\left(\frac{\omega m + kp_F - \frac{k^2}{2}}{\omega m}\right)$ . Going over under the cut of  $\ln(z'_1)$  we add the shift  $-2\pi i$  to the magnitude of  $\ln(z'_1)$ . Then, the logarithm on the sheet  $I'$  under the lower edge of the cut  $I'$  is equal to  $\ln\left(-\frac{\omega m + kp_F - \frac{k^2}{2}}{\omega m}\right) + \pi i - 2\pi i$ . This expression is used for the analytical continuation to the sheet  $I'$ . The part of the sheet  $I'$  is shown on the Fig.1c by the shading with the left slope.

The values of  $\Pi^{0R}(\omega, k)$  on the unphysical sheets  $I$  and  $I'$  defined by such a way are connected by the relation

$$\left(\Pi_I^{0R}(\omega, k)\right)^* = \Pi_{I'}^{0R}(-\omega^*, k). \quad (13)$$

Thus, we made two unphysical sheets  $I$  and  $I'$ . Let us show that the magnitudes of  $\Pi^{0R}(\omega, k)$  (4) on the negative imaginary axes of  $I$  and  $I'$  are real and are the same, according to (13). Then Eqs.(1), (12) and their solutions coincide as well.

On the imaginary axis we denote  $\omega = i\omega_i$ . On the sheet  $I$  the operator  $\Pi^{0R}(\omega, k)$  (4) has the following view on the negative imaginary axis

$$\Pi^{0R}(i\omega_i, k) = -\frac{mp_F}{\pi^2} \left[ 1 - \frac{i\omega_i m}{kp_F} \left( \ln \frac{-i\omega_i m}{i\omega_i m - kp_F + \frac{1}{2}k^2} - \pi i \right) \right. \quad (14)$$

$$\left. - \frac{i\omega_i m}{kp_F} \left( \ln \frac{i\omega_i m + kp_F - \frac{1}{2}k^2}{i\omega_i m} \right) + \dots \right].$$

$$= -\frac{mp_F}{\pi^2} \left[ 1 + 2 \frac{\omega_i m}{kp_F} \left( \arctg \frac{\omega_i m}{kp_F - \frac{1}{2}k^2} - \frac{\pi}{2} \right) + \dots \right]. \quad (15)$$

We leave only the first and the second terms in (5) because only these terms have the additional shifts on the sheets  $I$  and  $I'$ . This expression is the analytical continuation of  $\ln(-z_1) - \pi i$  to the imaginary axis.

On the negative imaginary axis of the sheet  $I'$  we have for  $\Pi^{0R}(\omega, k)$

$$\begin{aligned} \Pi^{0R}(i\omega_i, k) = & -\frac{mp_F}{\pi^2} \left[ 1 - \frac{i\omega_i m}{kp_F} \ln \frac{i\omega_i m}{i\omega_i m - kp_F + \frac{1}{2}k^2} \right. \\ & \left. - \frac{i\omega_i m}{kp_F} \left( \ln \frac{i\omega_i m + kp_F - \frac{1}{2}k^2}{-i\omega_i m} - \pi i \right) + \dots \right] \end{aligned} \quad (16)$$

and after the analogous transformation we obtain Eq.(15) as well.

We can conclude that there are unphysical sheets  $I$  and  $I'$ , that coincide on the imaginary axis. In the next section it is shown that the solutions of Eqs.(1), (12) at  $F_0 < 0$  are disposed on imaginary axes both of the physical and unphysical sheets.

### III.B Solution in the kinetic theory of Landau

At  $F_0 < -1$  the positive and negative symmetrical solutions to Eq.(12) are placed on the imaginary axis of the physical sheet ([2], [3]). These solutions satisfy to the equation which can be deduced from Eq.(12) ( $s = i\gamma$ )

$$1 + \frac{1}{F_0} = \gamma \operatorname{arctg} \frac{1}{\gamma}. \quad (17)$$

The existence of the amplified solutions means that there is an unstability of the nuclear matter.

Now we obtain the dispersion equation for the zero-sound excitations at  $-1 < F_0 < 0$ . We consider Eq.(15) at long wavelenths and then substitute it into Eq.(12). Then on the negative imaginary axis of the unphysical sheet we get an equation

$$1 + \frac{1}{F_0} = -\gamma(\operatorname{arctg}(\gamma) - \frac{\pi}{2}). \quad (18)$$

This equation was presented in [10] where it was mentioned that there are no actual solutions of (18). We really see that the solutions to Eq.(18) are placed on the unphysical sheet ( $I$ ).

In Fig.2 the solutions  $\gamma$  of Eq.(12) at  $F_0 < 0$  are presented. The curves in this figure are the same as the curves in Fig.1 in papers [10] and [6] (except the line  $AB$ ). The dashed domain means that the solutions are on the unphysical sheets. Looking at Fig.2 we see how the overdamping solutions on the unphysical sheet turn into the growing solutions and pass on to the physical sheet when the attraction between quasiparticles increases.

Using the unphysical sheets one may obtain the symmetric solutions at  $-1 < F_0 < 0$  (the line  $AB$ ). They are placed on the unphysical sheets ( $\tilde{I}$  and  $\tilde{I}'$ ) that are above the physical sheet. In appendix A the construction of these sheets is presented. In Fig.2 the horizontal shading marks the sheet  $\tilde{I}$ . The dispersion equation (12) on the unphysical positive imaginary axis has the same form on the sheets  $\tilde{I}$  and  $\tilde{I}'$ :

$$1 + \frac{1}{F_0} = -\gamma(\operatorname{arctg}(\gamma) + \frac{\pi}{2}). \quad (19)$$

This equation turns into Eq.(18) if to change the sign of  $\gamma$ . Solutions of this equation give the curve  $AB$  in Fig.2.

### III.C Solutions in RPA

In Fig.3 the solutions of Eq.(1) obtained in the kinetic theory of Landau and in RPA are shown simultaneously at  $F_0=-1.1, -1.2$ . The drawn solutions are on the upper semiplane of the physical sheet, i.e. they describe the unstable state of the nuclear matter.

The kinetic theory gives the linear dependence  $\omega \sim k$ , that shows the unlimited undamping increasing of the frequency with  $k$ . In RPA the dependence is different:  $Im\omega_{sd}(k)$  reach the maximum and then decrease. At a certain value of  $k$  (which we denote by  $k_{fin}$ ) the branch  $\omega_{sd}(k)$  goes over under the cut to the unphysical sheet  $I$ . The values of the maximum (which is proportional to the growth rate) and  $k_{fin}$  depend on parameters of matter  $F_0, p_F, m$ .

In Fig.4 the branches  $\omega_{sd}(k)$  obtained in RPA are presented. One sees that the branches change continuously with  $F_0$  passing from the physical to unphysical sheets  $I$ . At  $-1 < F_0 < 0$   $\omega_{sd}(k)$  are placed on the unphysical sheet completely. At  $F_0 < -1$  the branches lie on the physical sheet at the momenta  $k$  within the interval  $k = (0, k_{fin})$ . All solutions belong to the same family  $\omega_{sd}$ .

Similarly to Fig.2 the symmetrical branch  $-\omega_{sd}(k)$  can be found. At  $k = k_{fin}$  it goes over from the physical to unphysical sheets  $\tilde{I}$ .

There are two questions related to Fig.4. It is shown how the branch go over the cut to unphysical sheet  $I$  at  $k = k_{fin}$ . But the cuts  $I, I', \tilde{I}, \tilde{I}'$  exist when  $k \leq 2p_F$ . If  $\omega_{sd}(k)$  is on the unphysical sheet at  $k \approx 2p_F$ , where will it be at  $k > 2p_F$  when the cut is closed and teared off the physical sheet? One could show that  $\omega_{sd}(k)$  keep on to exist on the unphysical sheet.

The second question is what happens with  $\omega_{sd}(k)$  when  $k_{fin} > 2p_F$ ? This takes place when  $F_0 \ll -1$ . Looking at Fig.4 we wait that at  $k = k_{fin}$  the imaginary branch  $\omega_{sd}(k)$  go over to unphysical sheet but  $k_{fin} > 2p_F$  and the cut  $I$  is closed. At  $k_{fin} > 2p_F$  there are two cuts  $III$  and  $III'$  (8) on the real axis. They can be far from the point of origin if  $k_{fin}$  is distinctly larger  $2p_F$ . It can be shown that two imaginary branches  $\omega_{sd}(k)$  and  $-\omega_{sd}(k)$  turn to zero at  $k = k_{fin}$  and become real at  $k > k_{fin}$ . Further, as  $k$  increase they move along the real axis in the different sides, reach the cuts  $III$  and  $III'$  and go over under the cuts. This behaviour of branches is a standard one and is describe, for example, in [8].

### IV. Solutions at $F_0 > 0$

The existence of zero-sound collective excitations at the repulsive quasiparticle interaction  $F_0 > 0$  was predicted in the paper [1]. The solutions of Eq.(1) describing the zero-sound excitations in kinetic theory are presented in Fig.5. They are the same as in Fig.1 in papers [6] and [10].



In RPA zero-sound excitations are described by the solutions of Eq.(1). Usually they are denoted by  $\omega_s(k)$ . The excitations propagate with a small damping till the overlapping of the frequency  $\omega_s(k)$  with the frequency of the free particle-hole pairs. The overlapping takes place at a certain wave vector  $k$  that we denote  $k_d$ . It is  $k = k_d$  when the right point of the cut  $II$  meets  $\omega_s(k_d)$  [3]. For  $k > k_d$  the real solutions  $\omega_s(k)$  that correspond to the stable excitations, turn into the complex ones. These complex solutions describe the damping excitations and are situated on the unphysical sheet  $II$ , Fig.6.

The unphysical sheet  $II$  is made by the same way as in the previous section. The second logarithm in Eq.(5) has the value  $\ln(-z_2) + \pi i$ , where  $z_2 = \frac{\omega m - k p_F - \frac{1}{2}k^2}{\omega m - k p_F + \frac{1}{2}k^2}$ , on the upper edge of the cut  $II$  and  $\ln(-z_2) - \pi i$  on the lower edge. We define as the unphysical sheet  $II$  the sheet neighboring with the physical one where the magnitudes of  $\ln(z_2)$  differ by the quantity of  $+2\pi i$ . As before going over from the physical sheet to the sheet  $II$  we have the continues changes of  $\ln(z_2)$  and, consequently, of polarization operator.

In Fig.6 the sheet  $II$  is marked by the checked shading. In this figure  $\omega_s(k)$  is presented in the complex plane of  $\omega$ . At the wave vectors  $k < k_d$ , the real branch  $\omega_s(k)$  is on the real axis. At  $k = k_d$ ,  $\omega_s(k)$  becomes damping, goes over the cut to the sheet  $II$ .

In Fig.7 the different models of  $\omega_s(k)$  are compared. The results are obtained at  $F_0 = 2$ , the corresponding wave vector is  $\frac{k_d}{p_F} = 0.51$ . The solid line stands for the kinetic theory. The dashed lines are for the real and imaginary parts of  $\omega_s(k)$  in RPA. The imaginary part of excitations appears due to Landau damping [2].

The Landau damping can be calculated by the approximated equation [4]. Let us denote  $\omega_r = Re(\omega_s(k))$  and  $\omega_i = Im(\omega_s(k))$ . Then at  $\frac{\omega_i}{\omega_r} \ll 1$  the following approximate equation is valid

$$\omega_i = sign(\omega_r) Im \Pi^0(\omega_r, k) \left( \frac{\partial Re(\Pi^0)}{\partial \omega} \right)_{\omega=\omega_r}. \quad (20)$$

The  $\omega_i$  obtained with this equation is shown by the dotted line in Fig.7.

## V. Discussion

The effective quasiparticle interaction used in this paper is a simple constant interaction [5]

$$\mathcal{F} = C_0(F + F'(\vec{\tau}_1 \vec{\tau}_2) + G(\vec{\sigma}_1 \vec{\sigma}_2) + G'(\vec{\sigma}_1 \vec{\sigma}_2)(\vec{\tau}_1 \vec{\tau}_2)), \quad (21)$$

where  $\vec{\tau}, \vec{\sigma}$  are the isospin and spin Pauli matrices. The results presented above are the valid for all types of the interaction in Eq.(21): scalar, isospin, spin and spin-isospin one.

In the paper the unphysical sheets  $I$  and  $I'$  are defined. The family of the branches of solutions  $\omega_{sd}(k)$  is placed (partly) on the imaginary unphysical axis where these sheets coincide. It seems that the remaining surface of sheets is not use. But we can turn to the consideration of the pion dispersion equation [5] in the complex plane of  $\omega$ . This equation is closely connected with the zero-sound dispersion equation in the spin-isospin channel. It is appeared that the solutions responsible for the pion condensation are situated on the sheets  $I$  and  $I'$ . When these solutions at a certain conditions go over to the physical sheet

(analogously  $\omega_{sd}(k)$  in Fig.4) then the physical values become infinite. This is interpreted as a phase transition into another state containing the pion condensate in the ground state [5],[11].

The author thanks S.V. Tolokonnikov for the constructive critics and M.G.Ryskin for the fruitful discussions. The work is supported by the RFBR (a grant number 03-02-17724).

## Appendix A

Here we construct the unphysical sheets  $\tilde{I}$  and  $\tilde{I}'$ . The solutions of Eq.(5) that are presented by the curve  $AB$  in Fig.2 are placed on these sheets.

To pass on to the sheet  $\tilde{I}$  we do the analytical continuation in  $\omega$  of  $\ln(z) \equiv \ln\left(\frac{\omega m}{\omega m - kp_F + \frac{k^2}{2}}\right)$  from the lower edge of the cut  $I$  upwards, adding  $2\pi i$  to  $\ln(z)$ . The sheet  $\tilde{I}$  is situated above the physical sheet. The value of  $\ln\left(\frac{\omega m}{\omega m - kp_F + \frac{k^2}{2}}\right)$  above the upper edge of the cut  $I$  is  $\ln(-z) - \pi i + 2\pi i$ . This expression is continued on the sheet  $\tilde{I}$ .

In the similar way we construct the sheet  $\tilde{I}'$  making the analytical continuation of  $\ln(z') \equiv \ln\left(-\frac{\omega m + kp_F - \frac{k^2}{2}}{\omega m}\right)$  from the lower edge of cut  $I'$  adding  $2\pi i$  to logarithm.

## References

- [1] L.D.Landau, Sov.Phys.-JETP, **3**, (1957)920; Sov.Phys.-JETP, **5**, (1957)101.
- [2] L.D.Landau, E.M. Lifshitz, "*Statistical physics*" (Pergamon Press, 1989).
- [3] D.Pines, P.Nozieres "*The Theory of Quantum Liquids*" (W.A.Benjamin,Inc., 1966).
- [4] A.L. Fetter, J.D. Walecka, "*Quantum theory of many-particle systems*"(Mc-Graw-Hill, New York, 1971).
- [5] Migdal A.B.//Rev.Mod.Phys. 1978. V.50. P.107;  
A.B.Migdal,D.N.Voskresensky, E.E.Saperstein, and M.A. Troitsky, Phys.Rep. **192**(1990)179.
- [6] C.J. Pethick, D.G. Ravenhall, Ann. Phys. **183**, (1988), 131
- [7] H. Mueller, B.D. Serot , Phys. Rev. **C52** (1995) 2072.
- [8] J.R. Taylor, "*Scattering Theory*" (John Wiley, Inc. 1972); R.G. Newton *Scattering theory of waves and particles* (McGraw-Hill, 1967); P.D.B. Collins, E.J. Squires,"Regge poles and particle physics", (Springer-Verlag, Berlin, 1968).
- [9] E.G.Phillips "*Functions of a complex variable*" (Interscience Publisher Inc., New York, 1958).
- [10] M. Colonna, Ph. Chomaz, Phys. Rev. **49**, (1994) 1908.
- [11] Sadovnikova, M.G.Ryskin, Phys.At.Nucl. **64**(2001) 440.

# 1 Figure captions

Fig.1. a)The complex plane of frequency. The cuts of  $\Pi^{0R}$  Eq.(4) are shown. Numbers stand for the cuts (7). b)The complex plane of  $z_1$ . The cut corresponds to the cut  $I$  in Fig.a. c)The complex plane of frequency. The shading marks the unphysical sheets described in the text.

Fig.2. Solutions  $\omega_{sd}(k)$  to Eq.(12) at  $F_0 < 0$ . The variable  $\gamma$  is  $\gamma = \frac{m}{kp_F} Im \omega_{sd}$ . The shading with the right slope marks the unphysical sheet  $I$ . The horizontal shading marks the unphysical sheet  $\tilde{I}$ .

Fig.3. The comparison of the solutions in the kinetic theory and in the RPA. The solid (dashed) lines correspond to solutions obtained at  $F_0 = -1.2$  ( $F_0 = -1.1$ ).

Fig.4. The branches of solution  $\omega_{sd}(k)$  obtained in RPA at different values of  $F_0$ . The curve (1) corresponds to  $F_0 = -0.4$ ; (2)  $F_0 = -0.9$ ; (3)  $F_0 = -1.02$ ; (4)  $F_0 = -1.1$ ; (5)  $F_0 = -1.2$ . The shading marks the sheet  $I$ .

Fig.5. The solutions to Eq. (12)  $\omega_s$  at  $F_0 > 0$ . Two symmetric solutions are presented.

Fig.6. The complex plane of frequency. The solutions  $\omega_s(k)$  to Eq.(1) obtained in RPA are presented. The curve 1 is calculated at  $F_0 = 1$  and the curve 2 at  $F_0 = 2$ . The wave vector  $k_d$  marks the point when the Landau damping starts at this  $F_0$ :  $\frac{k_d}{p_F} = 0.13$  when  $F_0 = 1$ , and  $\frac{k_d}{p_F} = 0.52$  at  $F_0 = 2$ .

Fig.7. The branch  $\omega_s(k)$  at  $F_0 = 2$  is shown for the different models. The solid line is for the solutions of Eq.(12). The real  $\omega_r$  and the imaginary  $\omega_i$  parts of the RPA solutions are presented by the dashed curves. The dotted line stands for the  $\omega_i$  calculated by Eq.(20).

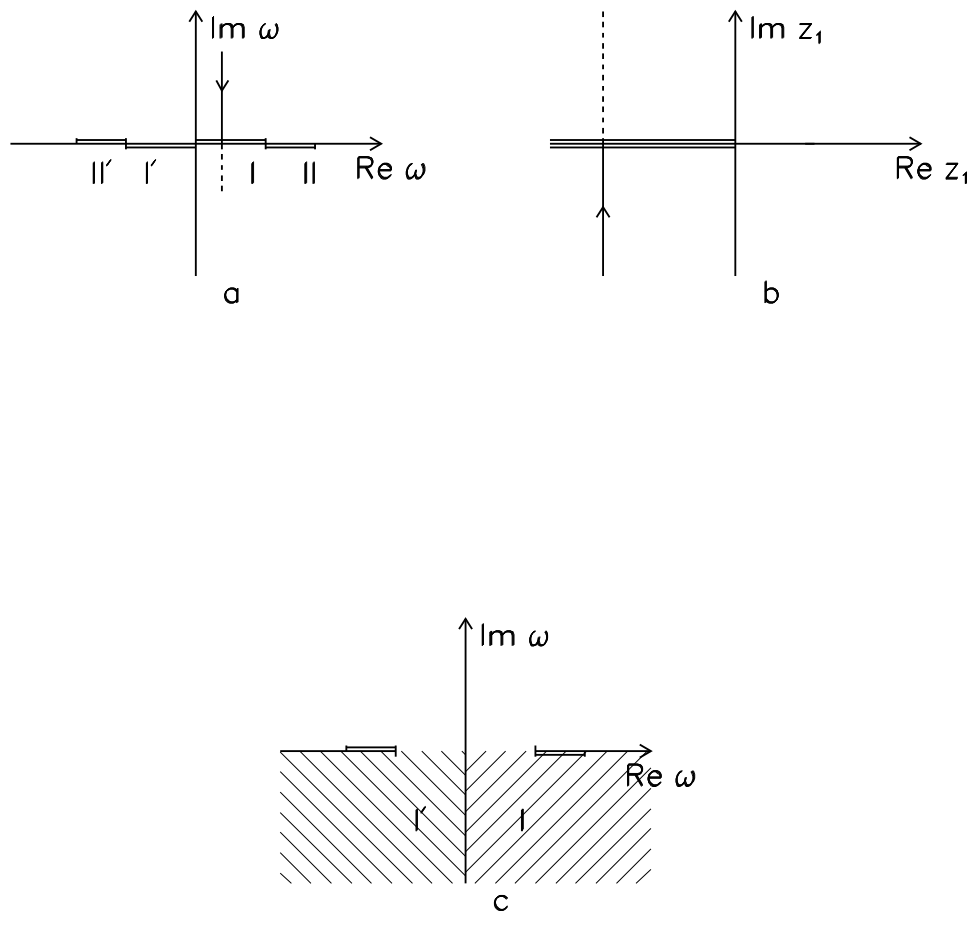


Figure 1:

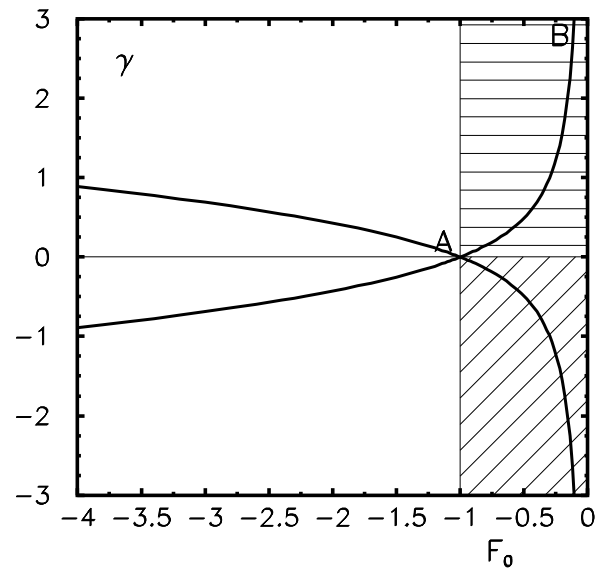


Figure 2:

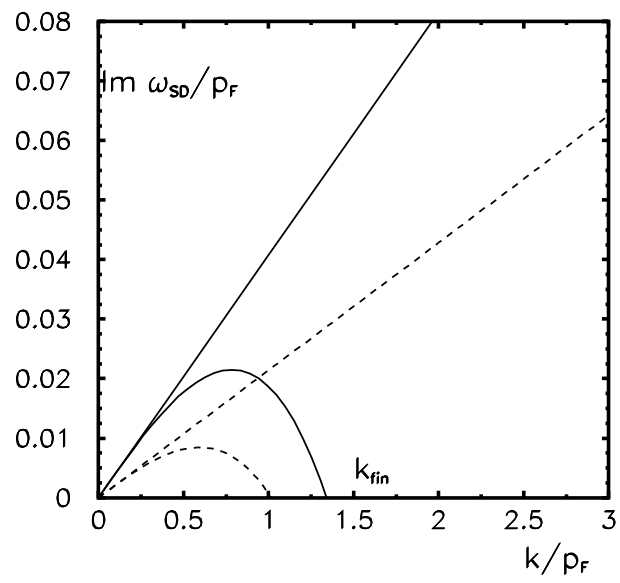


Figure 3:

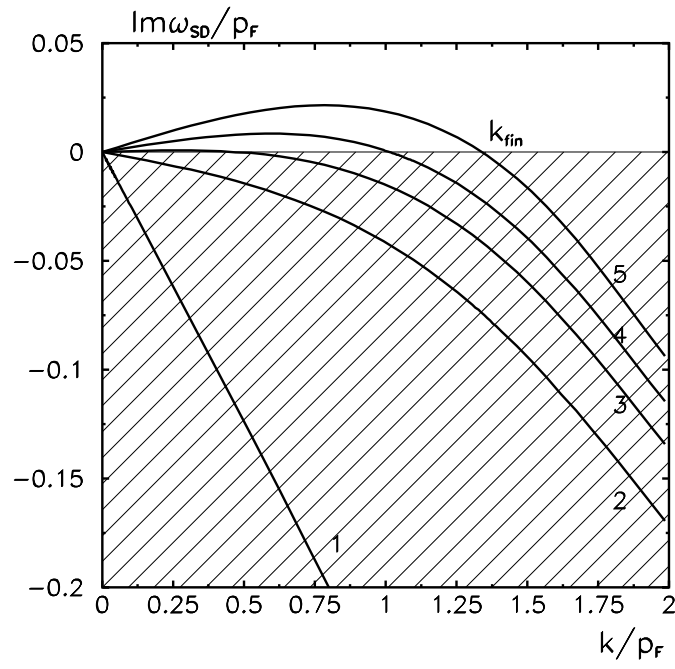


Figure 4:

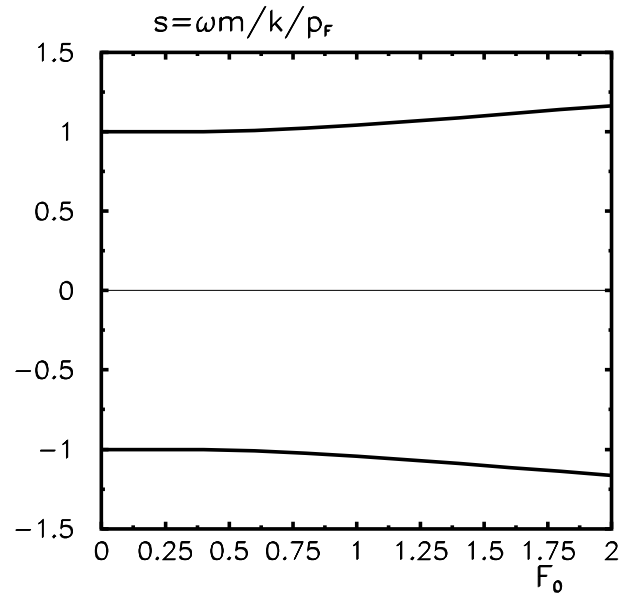


Figure 5:

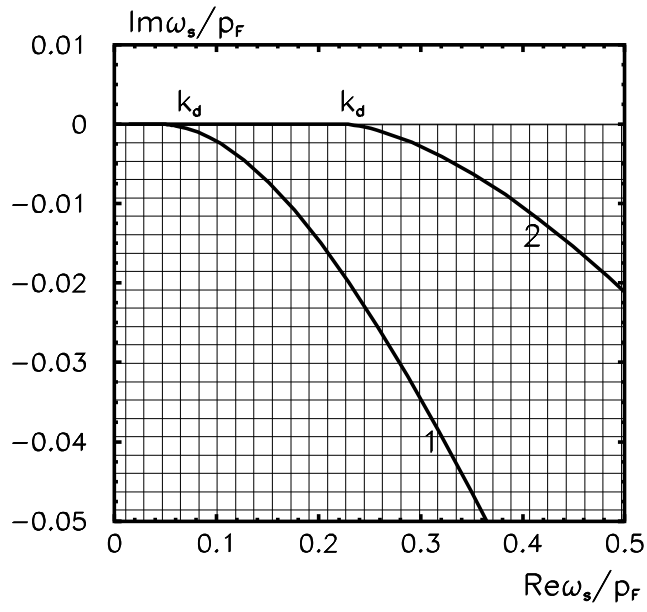


Figure 6:

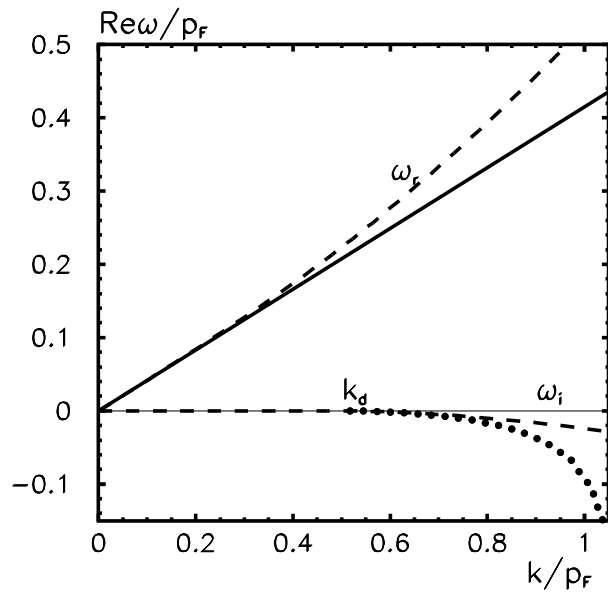


Figure 7: